Fish and Shellfish Immunology 92 (2019) 833–841

Contents lists available at ScienceDirect

Fish and Shellfish Immunology

journal homepage: www.elsevier.com/locate/fsi

Full length article

The role of infectious hematopoietic necrosis virus (IHNV) proteins in recruiting the ESCRT pathway through three ways in the host cells of fish during IHNV budding

Yaping Chen, Jiahui Li, Ying Zhou, Ying Feng, Xin Guan, Dechuan Li, Xuanyu Ren, Shuai Gao, Jinshan Huang, Xueting Guan, Wen Shi, Min Liu*

College of Animal Science and Technology, Northeast Agricultural University, Harbin, 150030, PR China

ARTICLE INFO

Keywords:
Infectious hematopoietic necrosis virus
Late-domain
ESCRT
Budding

ABSTRACT

In cytokinetic abscission, phagophore formation, and enveloped virus budding are mediated by the endosomal sorting complex required for transport (ESCRT). Many retroviruses and RNA viruses encode "late-domain" motifs that can interact with the components of the ESCRT pathway to mediate the viral assembly and budding. However, the rhabdovirus in fish has been rarely investigated. In this study, inhibition the protein expression of the ESCRT components reduces the extracellular virion production, which preliminarily indicates that the ESCRT pathway is involved in IHNV release. The respective interactions of IHNV proteins including M, G, L protein with Nedd4, Tsg101, and Alix suggest the underlying molecular mechanism by which IHNV gets access to the ESCRT pathway. These results are the first observation that rhabdovirus in fish gains access to the ESCRT pathway through three ways of interactions between viral proteins and host proteins. In addition, the results show that IHNV is released from host cells through the ESCRT pathway. Taken together, our study provides a theoretical basis for studying the budding mechanism of IHNV.

1. Introduction

The infectious hematopoietic necrosis virus (IHNV) is a member of the *Novirhabdovirus* genus in the *Rhabdoviridae* family of viruses [1]. Outbreaks of IHNV infection, leading to mass mortality, have posed a significant threat to the salmonid farming industry worldwide [2–5]. The IHNV has a negative-sense, single-stranded RNA genome of approximately 11 kilobases (kb), which encodes six proteins, including a nucleoprotein (N), a polymerase-associated phosphoprotein (P), a matrix protein(M), a unique glycoprotein (G), a large RNA-dependent RNA polymerase (L) [6–9] and a short gene located between the G and L genes that encodes a nonstructural nonvirion (NV) protein, which is a specific feature of *Novirhabdoviruses* [10–14]. The M protein has many different functions in the process of viral replication, among them the most important is the initiation of the assembly and budding of virions [15]. The stem budding domain of G protein promotes virus release by inducing membrane curvature at sites where virus budding occurs or by recruiting condensed nucleocapsids to sites on the plasma membrane which are competent for efficient virus budding [16]. However, the budding mechanism of IHNV in fish have largely remained obscure, understanding of which may be beneficial in developing more effective strategies for prevention against IHNV infection.

Most of the enveloped viruses acquire their envelope by budding from the cell membrane from being assembled inside the cell membrane, or assembled in the cytoplasm and transported to the inside of the cell membrane [17,18]. In recent years, it has been found that many proteins of the enveloped RNA viruses have a domain playing an important role in releasing virions from the cell membrane, known as late domains (L-domains), essential in the late steps of viral replication [19–26]. L-domains are binding sites for cellular factors facilitating viral budding [26]. There are now three distinct L domains identified and associated with budding defects within the retrovirus family, with core amino acid motifs of PT/SAP, PPXY, or YPXL/LXXLF [27–29]. The interaction between L domains and ESCRT components, including ESCRT-0, I, II, III, and VPS4 (Vacuolar protein sorting-associated protein 4) and Alix [ALP-2 (Apoptosis-linked gene 2)- interacting protein X] causes the virions to be released [30,31]. VPS4 is required for the budding of almost all viruses that are known to utilize the ESCRT pathway and appear to constitute the key machinery for budding [31]. Moreover, research shows that the PT/SAP motifs act by recruiting

* Corresponding author. College of Animal Science and Technology, Northeast Agricultural University, Chang Jiang Road No. 600, Xiang Fang District, Harbin, PR China. Tel.: +0086 15046005337.
E-mail address: liumin-707@163.com (M. Liu).

https://doi.org/10.1016/j.fsi.2019.07.011
Received 20 April 2019; Received in revised form 1 July 2019; Accepted 5 July 2019
Available online 09 July 2019
1050-4648/

Table 1
Summary of sequences used in this study. Italics and bold portion indicate enzyme sites for genetic tags. Underlined portion indicates point mutant sites. All primers used in this study were designed using Primer Premier 5.0.

Primer names	Primer sequences (5′-3′)
Expression vector	
IHNV M KpnF	***GGTACC***ATGTCCATTTTCAAGA
IHNV$M_{(PPPH-AAAA)}$ KpnF	***GGTACC***ATGTCCATTTTCAAGAGAGCAAAGAGAACAGTTCTGATCGCTGCTGCTGCC
IHNV M NotR	***GCGGCCGC***CTATTTTTCCTTCCCCCGTT
IHNV G Sal F	***GTCGAC***ATGGACGCCATGATCA
IHNV G Kpn R	***GGTACC***TTAGGACCTGTTTGCC
IHNV $G_{(PSAP-AARA)}$ Kpn R	***GGTACC***GGACCTGTTTGCCAGGTGATACATGGGGATACTCTGAGCCCGAGCAGC
IHNV L KpnF	GG***GGTACC***CCATGGACTTCTTCGAT
IHNV $L_{(LXXLF)}$1 R	AAATGGAGAGTCAGCTGCCGCGGCCGCGTCGGTTCTGA
IHNV $L_{(LXXLF)}$2 F	TCCAGAACCGACGCGGCCGCGGCAGCTGACTCTCCATTT
IHNV $L_{(LXXLF)}$2 R	GTCCAGTTTCTCGGCTGCGGCTGCGGCCGAGCTCTGTAG
IHNV $L_{(LXXLF)}$3 F	CTACAGAGCTCGGCCGCAGCCGCAGCCGAGAAACTGGC
IHNV $L_{(LXXLF)}$ Sal R	GC***GTCGAC***CTATTGTTCGCCTAGTGGAAAGAAGCC
Nedd4 Sal F	***GTCGAC****ATGTCAACAACGCGGCCCCT*
Nedd4 Nhe R	***GCTAGC***GCCTAGCAAAAGGCCCGATA
Tsg101 Kpn F	GG***GGTACC***ATGGCTGTTGTCAACGAAGG
Tsg101 Sal R	GC***GTCGAC***TCAGTATAGATCACTAAGTC
Alix Sal F	***GTCGAC***ATGGCGACGTTTATTTCTG
Alix-DN Sal F	***GTCGAC***ATGGTGTTGTTTAATGTGGG
Alix Kpn R	***GGTACC***CTGTTGGGGGTAATAGGGCT
RNA interfering	
siVPS4A	GCGAUUGAGCUGGUCACUATT
siVPS4B	CCAACAAUUCCACAUUCUUTT
siNedd4	GCAGCUUGCAGACCUGUAUTT
siTsg101	CCAUUCGAGCAUCACUAAUTT
qPCR	
IHNV–F	AGAGTTCGTGGAGGGGGTAGTC
IHNV-R	GGCAAGGAAGTCCGCATACG

ESCRT-I (endosomal sorting complex required for transport I) via a direct interaction with the ESCRT-I component Tsg101. Also, the LXXLF motif encoded within human immunodeficiency virus type 1 (HIV-1) p6 recruit AIP- 1/ALIX [29]. In addition, PPXY motifs in the L domains have been reported could bind to Nedd4-like E3 ubiquitin ligases and could induce the ubiquitination of a minimal HIV-1 Gag protein for facilitating viral budding [32,33]. However, the activation mechanism of ESCRT-III and the differences in the dependence of different viruses on ESCRT components remain unclear.

This study was undertaken to determine whether IHNV budding depends on the interaction between the L domains, PSAP, PPPH, LSKLF and LQDLF of the virus and the fish cells ESCRT components, and to explore further the budding of the virus to depend on the function of ESCRT components of the host cells. Our results provide a basis for understanding how the proteins of IHNV are recruiting the ESCRT pathway through three ways during budding, which may shed light on the prevention and control of IHNV infection in fish.

2. Materials and methods

2.1. Cells, viruses, plasmids, and antibodies

Chinook salmon embryo (CHSE-214) cells were obtained from the American Type Culture Collection (Manassas, VA, USA) and grown in L-15 (Leibovitz) supplemented media with 10% fetal bovine serum (FBS). The wild-type (wt) IHNV HLJ-09 viral strain (accession number JX649101) was generated in our laboratory and used in this study. The full-length genome plasmid pBlueScript II-IHNV HLJ-09 were designed in our laboratory [34]. Rabbit anti-IHNV and mouse anti-IHNV antibodies were prepared previously in our laboratory as previously described [35]. Anti-rabbit/mouse IgG (H + L)-HRP conjugates were purchased from Thermo Fisher Scientific (Waltham, MA) [14]. Mouse monoclonal antibody against the HA tag was purchased from Sigma (USA). Rabbit monoclonal anti-GAPDH antibody, rabbit monoclonal anti-β-actin antibody and rabbit monoclonal anti-Nedd4 antibody were purchased from CST (BRD). Rabbit monoclonal anti-Alix was obtained from Abcam (UK). Rabbit monoclonal anti-Tsg101, anti-VPS4B, and anti-VPS4A antibody were acquired from Bioss (China). All antibodies were used according to the manufacturers' instructions.

2.2. Plasmid construction and transient transfection

To research the role of IHNV L-domains, we analyzed the IHNV M, G and L contained the PPxY, PT/SAP or LXXLF domain, which was PPPH, PSAP, LSKLF and LQDLF by bioinformatics. Plasmids expressing IHNV L-domains proteins plasmids were constructed by reverse transcription-polymerase chain reaction amplification from the IHNV HLJ-09 strain genome. The mutate proline-proline-proline-histidine (PPPH) to alanine-alanine-alanine-alanine (AAAA) at position 14–17 of M protein was mutated using the overlapping extension PCR on the pBlueScript II-IHNV HLJ-09. Also, we mutated proline-serine-alanine-proline (PSAP) to alanine-alanine-arginine-alanine (AARA) at position 493–496 of G protein was mutated using the overlapping extension PCR on the pBlueScript II-IHNV HLJ-09. Then, we respectively mutated the leucine-serine-lysine-leucine-phenylalanine (LSKLF) and leucine-glutamine-asparagicacid-leucine-phenylalanine (LQDLF) to alanine-alanine-alanine-alanine-alanine (AAAAA) at position 942–946 and 1729–1733 of L protein used the sentence mentioned above methods. Moreover, we jointly mutated the two L-domains of L protein to AAAAA and named $L_{(LXXLF)}$. Plasmids expressing ESCRT proteins including Nedd4 (accession number NM_199787.2), Tsg101 (accession number NM_001002089.1) and Alix (accession number NM_213360.4) coding sequences were amplified via reverse transcription (RT)-PCR using a total RNA extract from CHSE-214 cells. Also, DN constructs of Alix were truncations of wild type (WT) Bro1 domain (residues 1–358), which served as the binding site for the ESCRT-III component with the virus [36]. All primers are shown in Table 1. The recombinant plasmids pCMV-HA-M, pCMV-HA-$M_{(PPPH-AAAA)}$, pCMV-HA-G, pCMV-HA-$G_{(PSAP-AARA)}$, pCMV-HA-L, pCMV-HA-$L_{(LXXLF)}$, pCMV-HA-Tsg101, pCMV-HA-Nedd4, pCMV-HA-Alix and pCMV-HA-Alix-DN were constructed using the pCMV-HA expression vector (Promega, Madison, WI, USA). All the clones were confirmed by restriction digestion and DNA sequencing.

Transient transfections of plasmids into CHSE-214 cells were performed using Lipofectamine LTX Plus (Life Technologies, USA) reagent according to the manufacturer's protocol.

2.3. Indirect immunofluorescence assay and western blotting

After CHSE-214 cells were transfected with various plasmids using the Lipofectamine LTX Plus reagent, the cells (cell confluency: 60–80%) were seeded on microscope coverslips placed in a 24-well plate for 48 h [37]. Uninfected cells were taken as negative. IFA was performed as described previously [38]. Also, the plasmid transfected cells were collected for SDS-PAGE analysis followed with western blotting, which was performed as described previously [14,38].

2.4. RNA interference

To confirm whether VPS4A (NM_001076609.1), VPS4B (NM_001291422.1), Nedd4 and Tsg101 functions in budding of IHNV, we silenced its expression in CHSE-214 cells. To this end, CHSE-214 cells were transfected with siVPS4A, siVPS4B, siNedd4 and siTsg101(GenePharma, China, sequences in Table 1). The siRNA against the green fluorescent protein (GFP) was synthesized as a negative control. siRNAs were transfected into cells at a final concentration of 100 nM using Hiperfect transfection reagent (Qiagen, BRD) [39].

2.5. Quantitative real-time PCR

To check the changes of mRNA abundance of targeting gene by qRT-PCR after siRNA transfection, CHSE-214 cells were transfected with 100 nM siRNA.The cells were cultured for 24 h, 48 h, 72 h, respectively. Then 250 μl of the extract was used for the extraction of total RNA by using an RNA extraction kit (Fastagen, China). Total RNA was reverse transcribed to cDNA, which was used for quantitative real-time PCR (qPCR). The assay ids of the PrimeTime Predesigned qPCR Assays used (Roche, CH) are shown in Supplementary Table S1. The experiments were carried out in triplicate. The housekeeping gene glyceraldehyde-3-phosphate dehydrogenase (GAPDH) was used for normalizing the amount of target mRNA. Relative mRNA expression was calculated using the $2^{-\Delta\Delta Ct}$ method (Supplementary Fig. S2) [14]. Also, CHSE-214 cells were transfected with 0.8 μg of Alix-DN plasmid or 100 nM siRNA for 6 h before infection with IHNV for 1 h. The cells were washed thrice with sodium citrate buffer. Then, fresh medium was added to the cells, and the cells were cultured for 66 h [39]. Then 1 ml of sterile PBS was added to homogenize the mixture, and 250 μl of the extract was used for the extraction of total RNA by using an RNA extraction kit (Fastagen, China). Total RNA was reverse transcribed to cDNA, which was used for absolute real-time qPCR (primer sequences in Table 1, accession number JX649101). Levels of IHNV GE were determined using Light Cycler 480 (Roche, CH). qPCR was carried out in triplicate per sample.

2.6. Electron microscopy

100 nM siVPS4A, siVPS4B, siNedd4, siTsg101, siGFP and 0.8 μg of Alix-DN plasmid and pCMV-HA plasmid were transfected into cells 6 h before infection with IHNV for 1 h. Moreover, the cells were washed thrice with sodium citrate buffer. Then, fresh medium was added to the cells, and the cells were cultured for 66 h. The cells were harvested as described previously, sectioned, and observed by electron microscopy (FEI, USA) [38].

2.7. Laser scanning confocal microscopy

CHSE-214 cells were transfected by recombinant plasmids pCMV-HA-Tsg101, pCMV-HA-Nedd4 and pCMV-HA-Alix for 24 h. Then, the cells were infected with IHNV. The cells were washed with sodium citrate buffer 1 h post infection to remove the unabsorbed virus, and the culture was replaced with fresh medium. The cells were incubated at 16 °C for 66 h. Samples were viewed under a confocal microscope (LSM510; Zeiss, GER) equipped with 647nm/488 nmlasers [39].

2.8. Co-immunoprecipitation

CHSE-214 cells were transfected with recombinant plasmids pCMV-HA-M, pCMV-HA-$M_{(PPPH-AAAA)}$, pCMV-HA-G, pCMV-HA-$G_{(PSAP-AARA)}$, pCMV-HA-L and pCMV-HA-$L_{(LXXLF)}$. After 48 h, the cells were lysed on ice with 1 ml of cell lysis buffer.

(Beyotime, China) for 30 min. The cell lysates were then centrifuged at 12 000 rpm for 10 min. A total of 600 μl of the supernatants at a final concentration of 3 μg/μl were respectively precipitated with anti-HA monoclonal antibody, anti-Nedd4 monoclonal antibody, anti-Tsg101 monoclonal antibody, anti-Alix monoclonal antibody in conjunction with Protein G Sepharose 4 Fast Flow (GE Healthcare Bio-Science, Piscataway, NJ) and were incubated with gentle rocking overnight at 4 °C. The beads were washed five times with cold IP buffer and boiled with 5xSDS loading buffer for 5 min. The immunoprecipitated proteins were detected by western blotting [38].

2.9. Statistical analysis

All experiments were performed at least three times with reproducible results. The Student's t-test was used to determine statistical significance. *P*-values of less than 0.05 were considered statistically significant, and those of less than 0.01 were considered highly significant.

3. Results

3.1. Expression of the proteins of IHNV and ESCRT components confirmed by IFA and WB

In order to verify the present monoclonal antibodies could react specifically with antigens of CHSE-214 cells and to determine the cross-reactivity of the antibodies against antigens in fish, Western blot analysis was performed by the extracts from the CHSE-214 cells and the HEK-293 cells using the anti-Tsg101, anti-VPS4B, anti-VPS4A, and anti-Nedd4 antibody as the primary antibody, and the cell lysates were used as the negative control. The results indicated that the present monoclonal antibodies could react specifically with antigens of CHSE-214 cells and there were the antibodies against antigens in fish and human (Supplementary Fig. S3). Also, to identify if the IHNV proteins and Nedd4, Tsg101, Alix have the respective interactions, ten plasmids expressing different proteins were constructed, respectively. Expression of each protein was confirmed by using IFA (Fig. 1A) and western blotting assay (Fig. 1B). Our results showed that all of the proteins of IHNV and ESCRT components could be efficiently and transiently expressed after plasmid transfection in the cells.

3.2. The role of VPS4 in IHNV budding

VPS4 expressing two closely related VPS4 proteins (A and B) in cells is necessary for budding of almost all proteins, the functions of which are interchangeable in some contexts [40]. To identify if VPS4 is important for efficient IHNV budding, we knocked down endogenous VPS4 expression by RNA interference. Fig. 2A showed that 100 nM siVPS4A caused a severe reduction in the expression levels of endogenous VPS4A from 24 h to 72 h. However, siGFP controlled displayed the almost identical expression levels from 24 h to 72 h during the budding process by western blotting analysis. Thus, based on absolute real-time quantitative PCR (qPCR) analysis, 100 nM siVPS4A and siGFP control were used to investigate whether exhaustion of endogenous proteins by siRNAs would reduce the production of IHNV

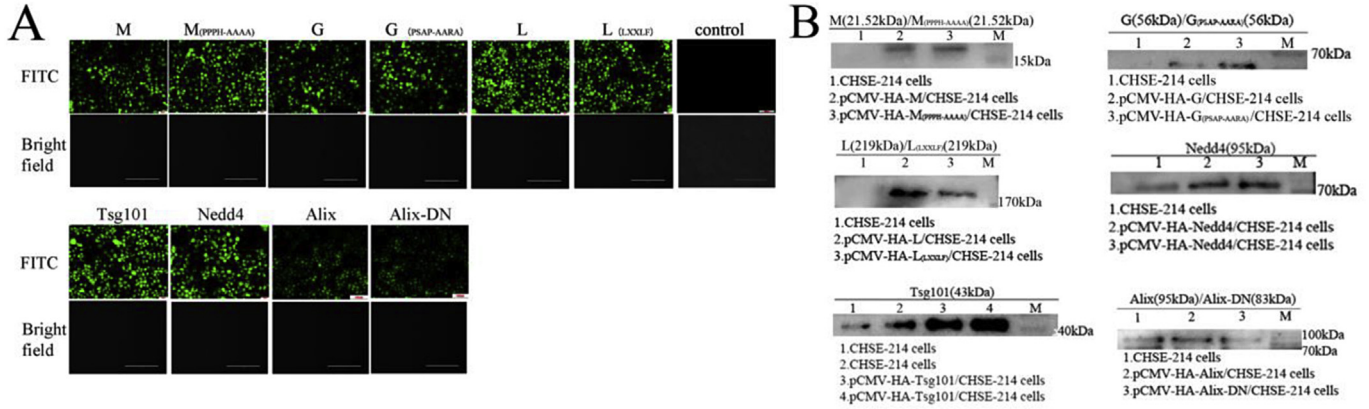

Fig. 1. All proteins expression were verified by transfection and detection by indirect immunofluorescence (A) and western blotting (B). CHSE-214 cells were transfected with indicated expression plasmids and pCMV-HA as the negative control, at 48 h post-infection, incubated with mouse-anti-IHNV serum (l:500) and rabbit-anti-Nedd4 (l:500), rabbit-anti-Tsg101 (l:500), rabbit-anti-Alix (l:500), then FITC-conjugated goat anti-mouse IgG (1:200) and FITC-conjugated goat anti-rabbit IgG (1:200) in turn. The cells were observed under a microscope. In addition, the plasmid transfected cells were collected for SDS-PAGE analysis followed with western blotting detection using mouse-anti-IHNV serum (l:200) and rabbit-anti-Nedd4 (l:200), rabbit-anti-Tsg101 (l:200), rabbit-anti-Alix (l:200), followed by HRP-conjugated goat anti-mouse IgG (1:5000) and FITC-conjugated goat anti-rabbit IgG (1:5000) at 48 h post-infection.

(Fig. 2B). Results showed that production levels of the extracellular IHNV particles and the production of the corresponding intracellular IHNV GEs transfected with siVPS4A and siGFP was not significantly different. Then, transmission electron microscopy was used to explore and visualize the IHNV-infected cells. Cells transfected with siVPS4A caused that the release of mature and enveloped virions was observed in the extracellular environment, which was no different compared with the siGFP control (Fig. 2C). The results showed that VPS4A did not play an important role in IHNV budding.

However, we verified the role of VPS4B with the same test method used for verifying VPS4A. The data were displayed differently. 100 nM siVPS4B caused a severe reduction in the expression levels of endogenous VPS4B from 24 h to 72 h (Fig. 3A) and production levels of the extracellular IHNV particles transfected with siVPS4B declined significantly, compared with those of the siGFP control, although the production of the corresponding intracellular IHNV GEs was not affected (Fig. 3B). Also, the intracellular unenveloped particles of the siGFP control were morphologically normal and displayed very few cell-associated virions and an abundance of released, mature, and enveloped virions were observed in the extracellular environment. Cells transfected with siVPS4B caused virus arrest at a very late stage during assembly. During this stage, extensive clusters of immature particles accumulated at the cell membrane by long membrane stalks, although the intracellular unenveloped particles were morphologically normal (Fig. 3C). In short, VPS4B was important for IHNV budding at a late stage of the virus life cycle.

3.3. Tsg101, Alix, and Nedd4 are functionally involved in IHNV budding

To investigate the roles of Tsg101, Alix, and Nedd4 in IHNV release, we used the analogous approaches described above. To study their effects on IHNV budding, CHSE-214 cells were transiently transfected with siTsg101 and siNedd4 to down-regulate the expression levels of Tsg101 and Nedd4. Figs. 4A and 5A showed that 100 nM siNedd4 and siTsg101 markedly reduced the expression levels of endogenous target proteins from 24 h to 72 h during the budding process. Simultaneously, Alix truncations expressed more proteins along with an increasing amount of plasmid (Fig. 6A). The highest plasmid concentrations were used to verify the role of the Alix protein. Then, we tested if the reduction in the IHNV production depended on the exhaustion of these endogenous proteins by 100 nM siTsg101 and siNedd4 or overexpression of Alix-DN truncations protein. The results indicated that

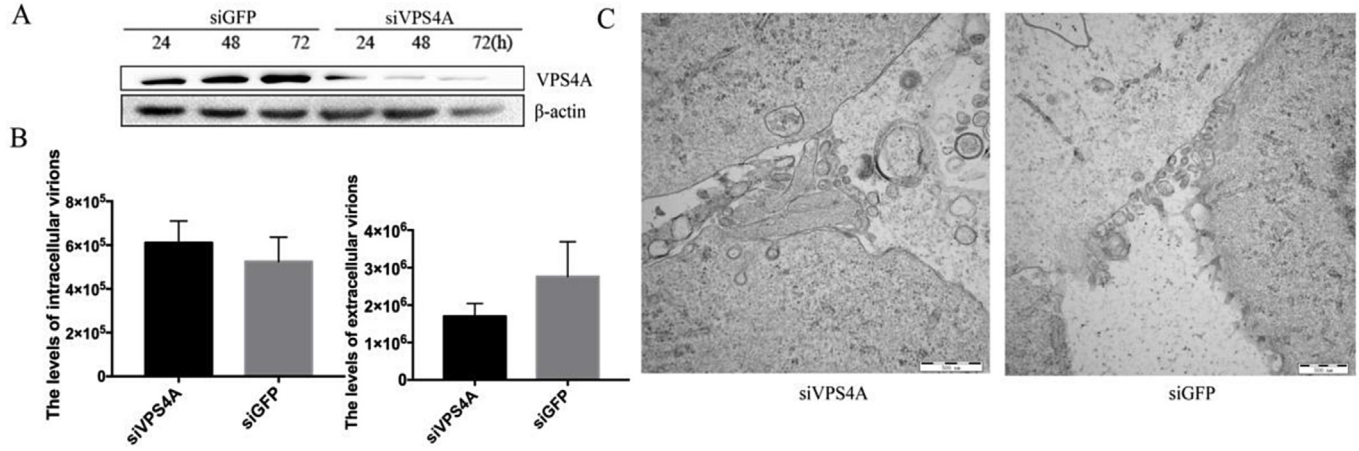

Fig. 2. The influences of production of the IHNV was whether mediated by RNA interference of VPS4A or not. (A) CHSE-214 cells were transfected by 100 nM of siRNA specific for VPS4A and control RNA (siGFP) The cells were collected from 24 h to 72 h and subjected to western blotting. (B) 100 nM siVPS4A or 100 nM siGFP were transfected into cells 6 h before infection with IHNV for 1 h and then cultured for 66 h. Cells and supernatant were lysed to extract DNA. Samples were then subjected to qPCR using IHNV primers to quantify IHNV genomic concentration. (C) EM analysis of CHSE-214 cells transfected with 100 nM siVPS4A or siGFP before infection with IHNV for 66 h.

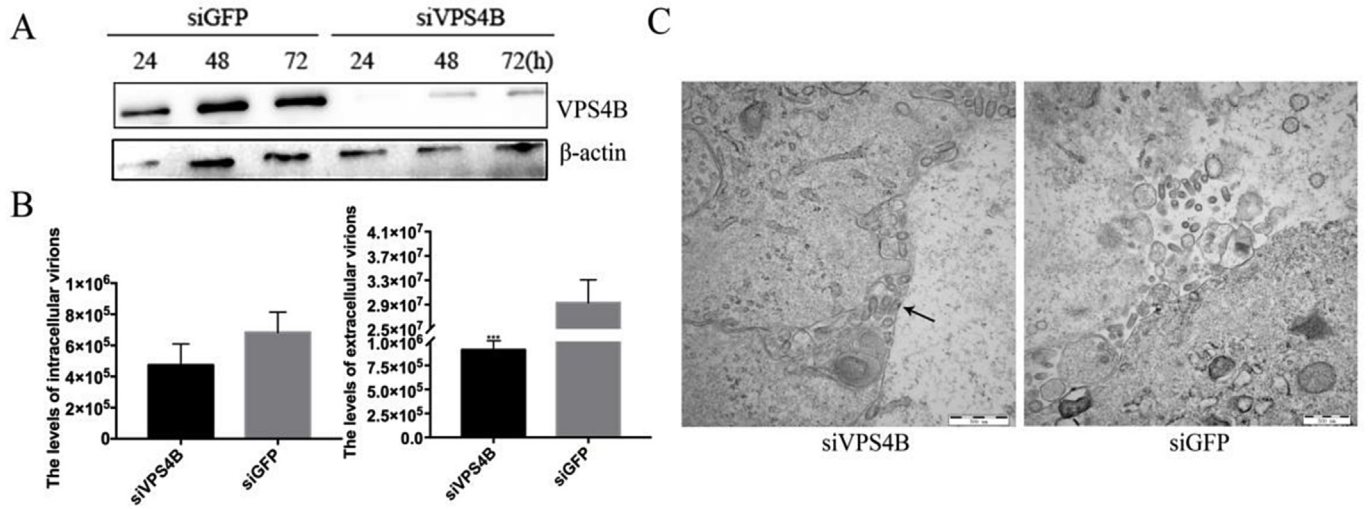

Fig. 3. Production of IHNV was inhibited by RNA interference of VPS4B. (A) CHSE-214 cells were transfected by 100 nM of siRNA specific for VPS4B and control RNA (siGFP). The cells were collected from 24 h to 72 h and subjected to western blotting. (B) 100 nM siVPS4B or 100 nM siGFP were transfected into cells 6 h prior to infection with IHNV for 1 h and then cultured for 66 h. Cells and supernatant were lysed to extract DNA. Samples were then subjected to qPCR using IHNV primers to quantify IHNV genomic concentration. Statistical analysis was performed using Student's t-test (*$p < 0.05$, **$p < 0.01$, ***$p < 0.001$). (C) EM analysis of CHSE-214 cells transfected with 100 nM siVPS4B or siGFP prior to infection with IHNV for 66 h. Arrows indicated virions tethered to the plasma membrane.

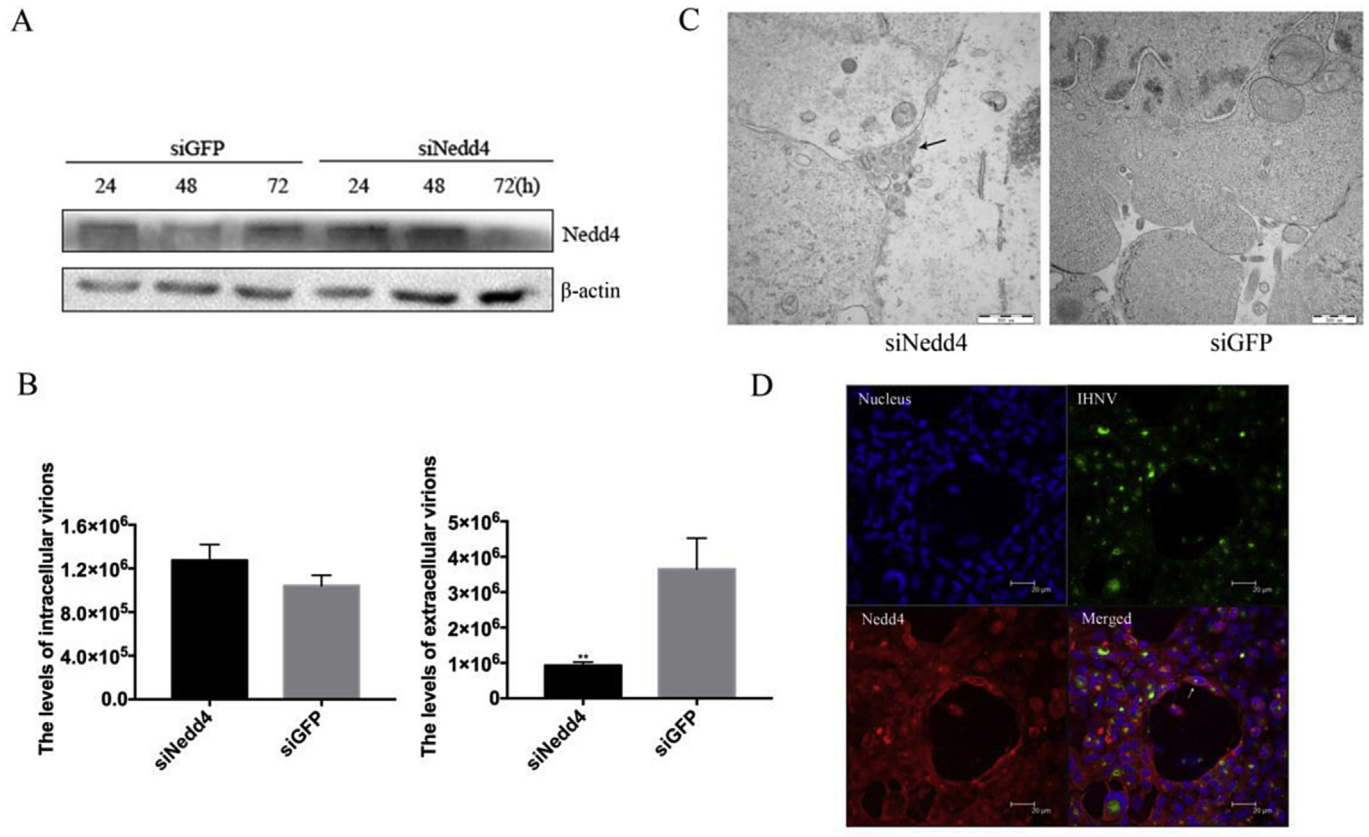

Fig. 4. Production of IHNV was inhibited by RNA interference of Nedd4. (A) 100 nM siNedd4 and control RNA (siGFP) were transfected into cells. The cells were collected from 24 h to 72 h and then subjected to western blotting. (B) 100 nM siNedd4 or 100 nM siGFP were transfected into cells 6 h before infection with IHNV for 1 h and then cultured for 66 h. Cells and supernatant were lysed to extract DNA. Samples were then subjected to qPCR using IHNV primers to quantify IHNV genomic concentration. Statistical analysis was performed using Student's t-test (*$p < 0.05$, **$p < 0.01$, ***$p < 0.001$). (C) EM analysis of CHSE-214 cells transfected with 100 nM siNedd4 or siGFP before infection with IHNV for 66 h. Arrows indicated virions tethered to the plasma membrane. (D) In vivo confocal microscopy analysis was performed after CHSE-214 cells were infected with IHNV for 1 h and cultured for 66 h. Cells were processed for immunostaining as described under “Materials and Methods”. Arrows indicate co-localization of IHNV and endogenous Nedd4.

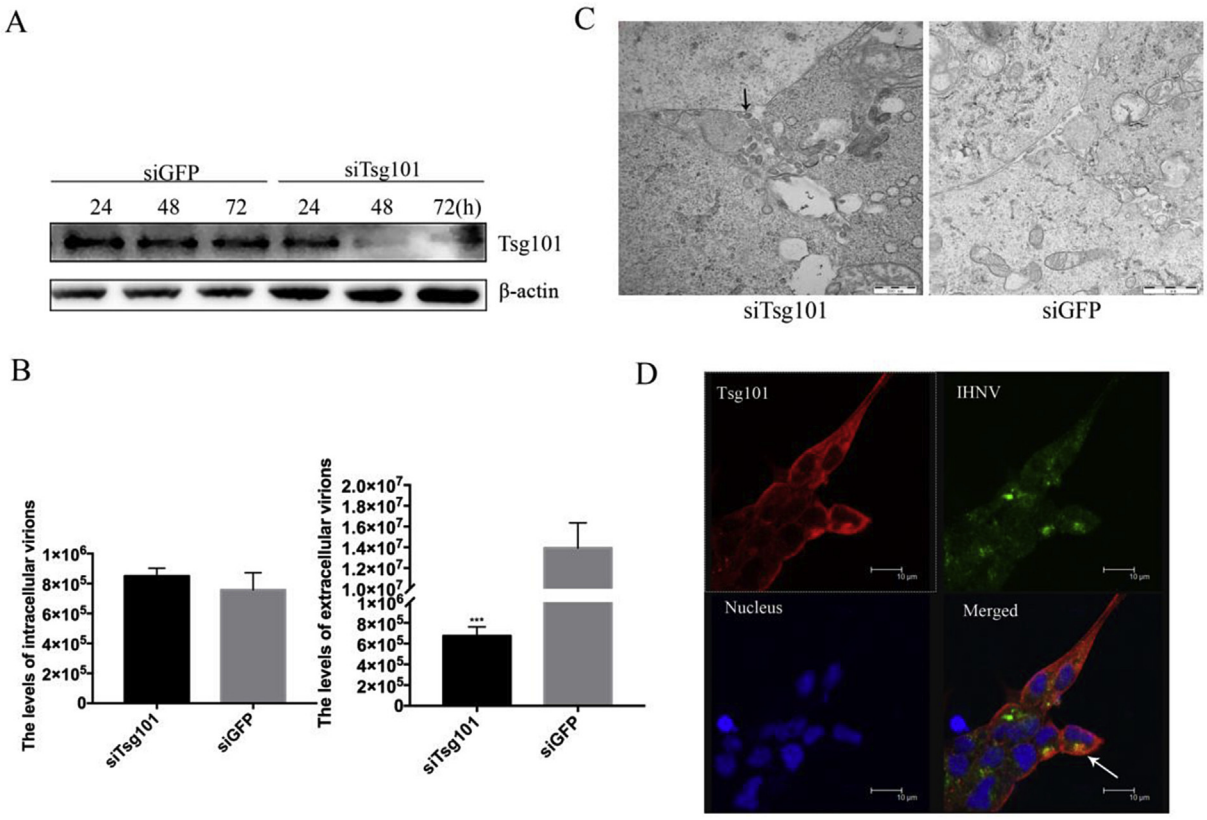

Fig. 5. Production of IHNV was inhibited by RNA interference of Tsg101. (A) 100 nM siTsg101 and control RNA (siGFP) were transfected into cells. The cells were collected from 24 h to 72 h and then subjected to western blotting. (B) 100 nM siTsg101 or 100 nM siGFP were transfected into cells 6 h before infection with IHNV for 1 h and then cultured for 66 h. Cells and supernatant were lysed to extract DNA. Samples were then subjected to qPCR using IHNV primers to quantify IHNV genomic concentration. Statistical analysis was performed using Student's t-test (*$p < 0.05$, **$p < 0.01$, ***$p < 0.001$). (C) EM analysis of CHSE-214 cells transfected with 100 nM siTsg101 or siGFP before infection with IHNV for 66 h. Arrows indicated virions tethered to the plasma membrane. (D) In vivo confocal microscopy analysis was performed after CHSE-214 cells were infected with IHNV for 1 h and cultured for 66 h. Cells were processed for immunostaining as described under "Materials and Methods". Arrows indicate co-localization of IHNV and endogenous Tsg101.

compared with the siGFP control, the extracellular IHNV particle productions were significantly decreased after transfection of siNedd4 and siTsg101, respectively (Figs. 4B and 5B). Correspondingly, the extracellular IHNV particle productions were significantly decreased on cells transfected by Alix-DN, compared with transfection of pCMV-HA (Fig. 6B). The data illustrated that loss of Alix, Tsg101, and Nedd4 compromised viral budding.

Also, cells transfected with 100 nM siNedd4, siTsg101 and 0.8 μg of Alix-DN plasmid caused virus arrest at a very late stage during assembly (Figs. 4C, 5C and 6C). In short, Nedd4, Tsg101 and Alix were important for IHNV budding at a late stage of the virus life cycle.

To confirm whether IHNV recruited Nedd4, Tsg101 and Alix to facilitate budding, we utilized the laser scanning confocal microscopy. Moreover, we assigned anti-IHNV as the marker of the IHNV particle and monoclonal anti-Nedd4, anti-Tsg101, anti-Alix as the marker of their proteins. The data revealed that the overlay of the fluorescence patterns revealed extensive co-localization of IHNV with Nedd4, Tsg101 and Alix and (Figs. 4D, 5D and 6D), which demonstrated that Nedd4, Tsg101 and Alix were recruited to the budding site to facilitate virus release.

3.4. IHNV L-domains contained proteins interact with Nedd4, Tsg101 and Alix

We verified whether L-domains could interact with the host ESCRT proteins by immunoprecipitation, the results showed that Nedd4 protein was detected after the anti-HA antibody was used to immunoprecipitate endogenous M (Fig. 7A, lane 5, top), and no band was detected when pCMV-HA was transfected as control vector (Fig. 7A, lane 6, top). Nedd4 protein was not detected after the anti-HA antibody was used to immunoprecipitate endogenous $M_{(PPPH\text{-}AAAA)}$ (Fig. 7A, lane 4, top). Then, we discovered that M could be detected after using an anti-Nedd4 antibody to immunoprecipitate endogenous Nedd4 (Fig. 7A, lane 5, bottom), and no band was detected when the CHSE-214 cells were transfected with pCMV-HA-$M_{(PPPH\text{-}AAAA)}$ and pCMV-HA and (Fig. 7A, lane 4 and 6, bottom). Similarly, the results indicated that Tsg101 protein was detected after the anti-HA antibody was used to immunoprecipitate endogenous G (Fig. 7B, lane 5, top), and no band was detected when the CHSE-214 cells were transfected with pCMV-HA-$G_{(PSAP\text{-}AARA)}$ and pCMV-HA (Fig. 7B, lane 4 and 6, top). Thus, we discovered that G could be detected after using an anti-Tsg101 antibody to immunoprecipitate endogenous Tsg101 (Fig. 7B, lane 5, bottom), and no band was detected when pCMV-HA was transfected as control vector (Fig. 7B, lane 6, bottom). $G_{(PSAP\text{-}AARA)}$ was not detected after the anti-Tsg101 antibody was used to immunoprecipitate endogenous Tsg101 (Fig. 7B, lane 4, bottom). Similarly, the results showed that Alix protein was detected after the anti-HA antibody was used to immunoprecipitate endogenous L (Fig. 7C, lane 5, top), and no band was detected when pCMV-HA was transfected as control vector (Fig. 7C, lane 6, top). Alix protein was not detected after the anti-HA antibody was used to immunoprecipitate endogenous $L_{(LXXLF)}$ (Fig. 7C, lane 4, top). Then, we discovered that L could be detected after using anti-Alix antibody to immunoprecipitate endogenous Alix (Fig. 7C, lane 5, bottom), and no band was detected when the CHSE-214 cells were transfected with pCMV-HA- $L_{(LXXLF)}$ and pCMV-HA (Fig. 7C, lane 4 and 6, bottom).

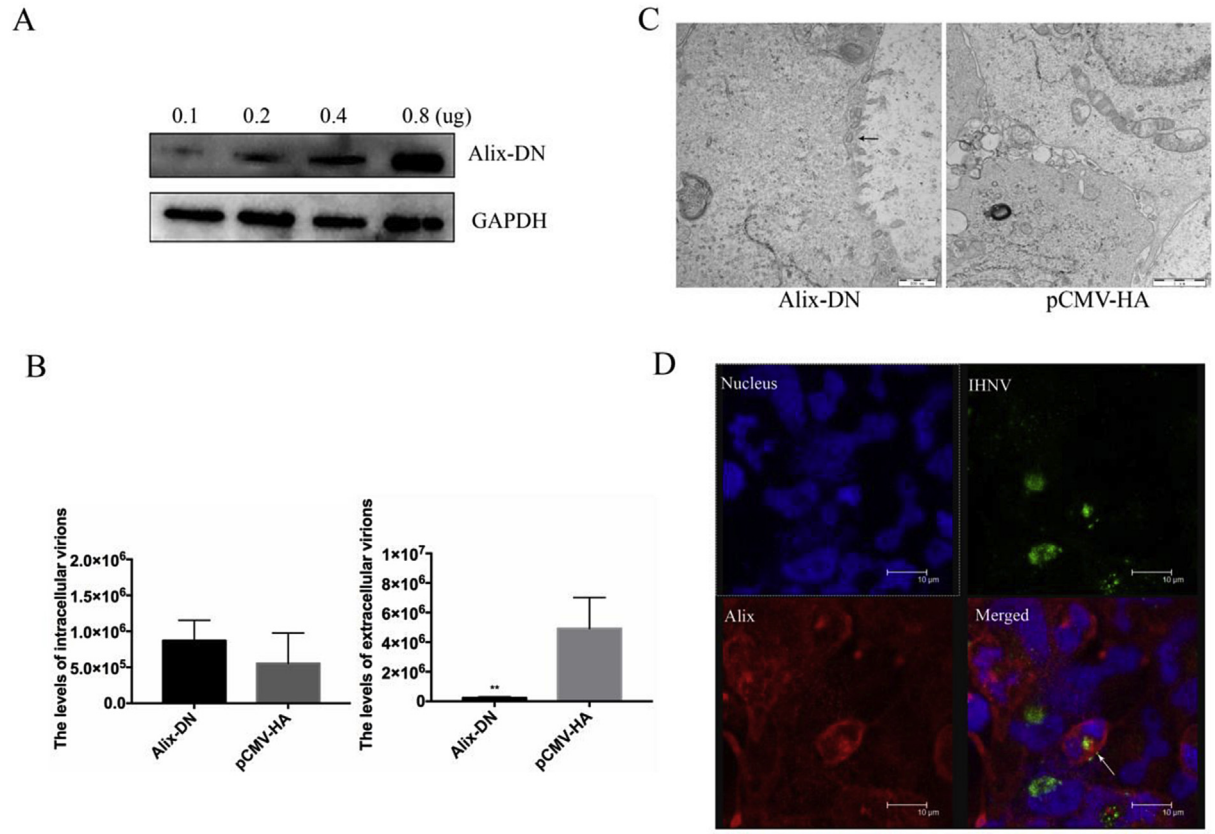

Fig. 6. Production of IHNV was inhibited by Alix-DN. (A) CHSE-214 cells were transfected with 0.1, 0.2, 0.4, or 0.8 μg of pCMV-HA-Alix-DN. Protein samples were collected and analyzed by western blotting, and GAPDH was included as control. (B) CHSE-214 cells were infected with IHNV for 1 h after transfection with 0.8 μg of pCMV-HA-Alix-DN or pCMV-HA and then cultured for 66 h. Cells and supernatant were lysed to extract DNA. Samples were then subjected to qPCR using IHNV primers to quantify IHNV genomic concentration. Statistical analysis was performed using Student's t-test (*$p < 0.05$, **$p < 0.01$, ***$p < 0.001$). (C) EM analysis of CHSE-214 cells transfected with 0.8 μg of pCMV-HA-Alix-DN or pCMV-HA before infection with IHNV for 66 h. Arrows indicated virions tethered to the plasma membrane. (D) In vivo confocal microscopy analysis was performed after CHSE-214 cells were infected with IHNV for 1 h and cultured for 66 h. Cells were processed for immunostaining as described under "Materials and Methods". Arrows indicate co-localization of IHNV and endogenous Alix.

We respectively tested whether the LSKLF and the LQDLF at position 942–946 and 1729–1733 of L proteins had the interaction with Alix. The results show that there is interaction among them (data unshown). Also, we repeatedly tested whether the viral proteins containing putative L-domains interacted with endogenous corresponding host proteins by many immunoprecipitation experiments. We found that the three viral proteins could directly interact with Alix, Tsg101, and Nedd4. Furthermore, there were no bands when we verified point mutant L-domains with immunoprecipitation experiments, which showed that the L-domain played roles in these interactions. These binding interactions represent the mechanism by which IHNV recruits ESCRT pathway for budding.

4. Discussion

The envelope virus buds out of the cytoplasmic membrane of the infected cells and acquires a capsule. Most enveloped viruses' bud and release invasive progeny virions of the final neck shear stage by plundering the host cell plasma membrane share device ESCRT system. The L-domain motif is capable of binding to different host ESCRT proteins to accomplish budding and release of the virus [18]. In this study, IHNV relied on the network of ESCRT proteins to complete virus budding. The present work was the first to report an example of the budding mechanism of IHNV. Also, results showed that three approaches were used to access the pathway, and all these approaches contributed to complete virus budding (Fig. 8).

VPS4 is a member of AAA (ATPases associated with diverse Cellular activities) ATPase family and the only ATPase in the MVB pathway [41], which could dissociate ESCRT complexes for recycling by providing energy with hydrolysis of ATP. VPS4 plays an important role in the MVB pathway, cytokinesis, and virus budding. Results from early studies suggested that host protein VPS4 and the ESCRT pathway may not be important for budding of rhabdoviruses, however, subsequent studies using stable cell lines expressing VPS4 suggest that there is a role for the ESCRT machinery in rhabdoviral egress [42]. In this study, we first detected the role of VPS4 in IHNV budding. The data showed that VPS4B down-regulated by siRNA silencing caused the marked effect of IHNV budding. However, there was no significant effect of causing IHNV budding under VPS4A down-regulation. These results indicated that VPS4B played an important role in IHNV budding. Moreover, VPS4A did not seem to be necessary for IHNV budding. Thus, the role of VPS4A in IHNV needs further investigation.

Different viral proteins displayed in different ways to recruit the ESCRT pathway. Research reports emphasize the concerted contributions of both M and G proteins in RABV assembly and egress [43]. IHNV and RABV are parts of the enveloped virus and belong to the Rhabdoviridae family. All of these viral proteins including the presence of one or more domains referred to as "late" budding domains (L-domains), which interacts with a specific host protein of ESCRT pathway to promote virus budding [44]. Tsg101 is a component of ESCRT-I [45], which is an essential cellular complex in the ESCRT pathway and which can restrict constitutive NF-kB signaling by preventing the accumulation and activation of NF-kB–inducing receptors [46]. In this study, we inhibited the proteins of Nedd4 and Tsg101 by reducing extracellular

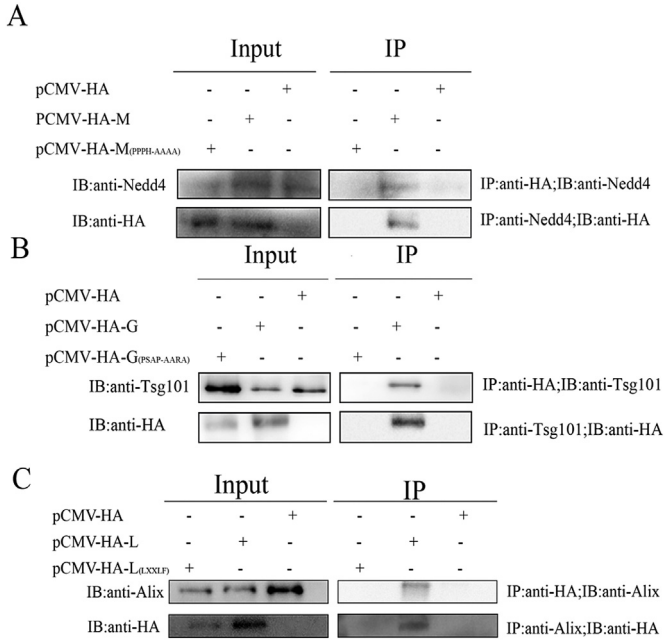

Fig. 7. Identification of the protein–protein interaction between IHNV protein containing putative L-domain and corresponding host protein using immunoprecipitation (IP). (A)IP of M and Nedd4 using anti-HA antibody and anti-Nedd4 antibody. CHSE-214 cells were transfected with pCMV-HA-M, pCMV-HA- M(PPPH-AAAA) or an empty vector pCMV-HA. Cells were processed for IP as described under "Materials and Methods". Anti-Nedd4 antibody and anti-HA antibody were used as the primary antibodies for IP. (B) IP of G and Tsg101 using anti-HA antibody and anti-Tsg101 antibody. CHSE-214 cells were transfected with pCMV-HA-G, pCMV-HA- G (PSAP-AARA) or an empty vector pCMV-HA. Cells were processed for IP as described under "Materials and Methods". Anti-Tsg101 antibody and anti-HA antibody were used as the primary antibodies for IP. (C) IP of L and Alix using anti-HA antibody and anti-Alix antibody. CHSE-214 cells were transfected with pCMV-HA-L, pCMV-HA- L (LXXLF) or an empty vector pCMV-HA. Cells were processed for IP as described under "Materials and Methods". Anti-Alix antibody and anti-HA antibody were used as the primary antibodies for IP.

virion production, which preliminarily indicates that Nedd4 and Tsg101 are involved in IHNV release. However, the role of Tsg101 for NF-kB about the immune system in fish cells remains to be further investigated. Moreover, Alix-Bro1 domain served as the binding site for the ESCRT-III component with the virus. Thus, we tested Alix DN mutants, lacking the Alix-Bro1 domain, suppressed IHNV production, which illustrated that Alix is involved in IHNV release. Also, we repeatedly tested whether the viral proteins containing putative L-domains interacted with the endogenous corresponding host proteins by many immunoprecipitation experiments. We found that the M, G, L proteins of IHNV could directly interact with Nedd4, Tsg101, and Alix. Taken together, the interactions between viral proteins bearing L-domains and their corresponding class E proteins were important for IHNV budding, and the involved host factors all had roles in IHNV budding.

The majority of RNA viruses express one or two L-domains in a specific protein, and the use of two distinct L-domains have equivalent and therefore redundant functions in virus release [47]. The HIV-1 Gag protein contained the PTAP and YPXnL domains and blocked PTAP-Tsg101 or YPXnL-Alix interactions both affected HIV-1 release [36]. Also, HSV-1 encoded all three classes of L-domains in several structural proteins and required functional ESCRT III complex and VPS4 but independent of Tsg101 and Alix [48]. In our study, there were no bands when we verified point mutant L-domains with immunoprecipitation experiments, which showed that the L-domain played roles in these interactions. These data suggested that the PPPH, PSAP or LXXLF motifs of IHNV proteins play an essential role during the virus budding. Moreover, we analyzed the effects of simultaneous depletion of multiple proteins with various combinations. The results that such functional redundancy may allow for the loss of one or two interactions between L-domain contained viral proteins or corresponding host proteins (data not shown). These results indicated that a number of parallel mechanisms by which IHNV could access the ESCRT machinery are redundant; any of these approaches could, to some extent, be sufficient for virus budding. In addition, three L-domains were located in different viral proteins, indicating that defects in one or two viral proteins or loss of any relevant factors in host cells could not completely block IHNV propagation and may be associated with broad range of cell lines that allow IHNV infection [49].

In summary, we first confirmed that there were ESCRT components in fish host cells that interact with the PPPH, PSAP or LXXLF motifs of

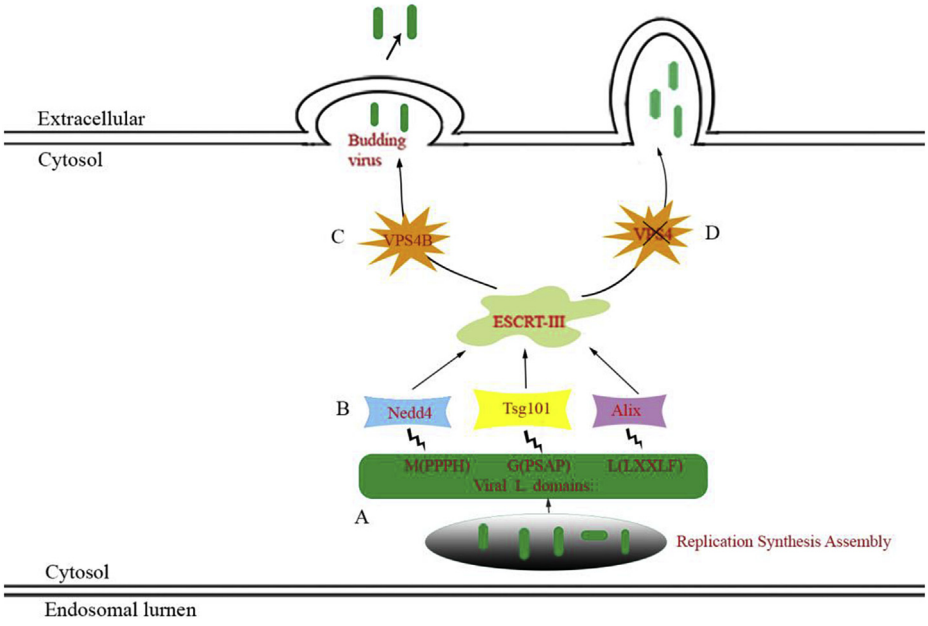

Fig. 8. Model of cellular budding of IHNV. (A) IHNV replicates and assembles at the nucleus and cytoplasm. (B) IHNV gains access to ESCRT pathway through three ways of interactions between viral proteins and host proteins. (C) VPS4B functions in budding and formation of mature enveloped virus particles. (D) Loss of VPS4 leads to defective budding.

IHNV proteins, which recruits the ESCRT pathway to mediate virus budding. Viruses employ the same pathway to complete budding, but the cellular locations at which the viral proteins assemble vary. Thus, the detailed biological mechanisms involved in the IHNV cellular locations at which the viral proteins assembled for budding remains to be further investigated.

Acknowledgements

This work was supported by the National Natural Science Foundation of China (Grant No.31672697; 31372568) and national natural fund international cooperation program(No.31511130137).

Appendix A. Supplementary data

Supplementary data to this article can be found online at https://doi.org/10.1016/j.fsi.2019.07.011.

References

[1] S. Ahmadivand, M. Soltani, K. Mardani, S. Shokrpoor, R. Hassanzadeh, M. Ahmadpoor, et al., Infectious hematopoietic necrosis virus (IHNV) outbreak in farmed rainbow trout in Iran: viral isolation, pathological findings, molecular confirmation, and genetic analysis, Virus Res. 229 (2017) 17–23.
[2] R.R. Rucker, W.J. Whipple, J.R. Parvin, C.A. Evans, A Contagious Disease of Salmon Possibly of Virus Origin vol. 76, Washington the Service Usgovt Printoff, 1953.
[3] M.K. Purcell, S.E. Lapatra, J.C. Woodson, G. Kurath, J.R. Winton, Early viral replication and induced or constitutive immunity in rainbow trout families with differential resistance to Infectious hematopoietic necrosis virus (IHNV), Fish Shellfish Immunol. 28 (2012) 98–105.
[4] L.R. Pierce, C.A. Stepien, Evolution and biogeography of an emerging quasis-pecies: diversity patterns of the fish Viral Hemorrhagic Septicemia virus (VHSV), Mol. Phylogenetics Evol. 63 (2012) 327–341.
[5] S.L. Rudakova, G. Kurath, E.V. Bochkova, Occurrence and genetic typing of infectious hematopoietic necrosis virus in Kamchatka, Russ. Dis. Aquat. Org 75 (2007) 1–11.
[6] S.P. Morzunov, J.R. Winton, S.T. Nichol, The complete genome structure and phylogenetic relationship of infectious hematopoietic necrosis virus, Virus Res. 38 (1995) 175–192.
[7] R. Assenberg, O. Delmas, B. Morin, S.C. Graham, X.D. Lamballerie, et al., Genomics and structure function studies of Rhabdoviridae proteins involved in replication and transcription, Antivir. Res. 87 (2010) 149–161.
[8] M.S. Kim, K.H. Kim, Protection of olive flounder, Paralichthys olivaceus, against viral hemorrhagic septicemia virus (VHSV) by immunization with NV gene-knockout recombinant VHSV, Aquaculture 314 (2011) 39–43.
[9] P. Pereiro, A.M. Lopez, A. Falco, S. Dios, A. Figueras, J.M. Coll, B. Novoa, A. Estepa, Protection and antibody response induced by intramuscular DNA vaccine encoding for viral haemorrhagic septicaemia virus (VHSV) G glyco- protein in turbot (Scophthalmus maximus), Fish Shellfish Immunol. 32 (2012) 1088–1094.
[10] A. Ammayappan, V.N. Vakharia, Nonvirion protein of novirhabdovirus suppresses apoptosis at the early stage of virus infection, J. Virol. 85 (2011) 8393–8402.
[11] S. Biacchesi, M.I. Thoulouze, M. Bearzottim, Y.X. Yu, M. Bremont, Recovery of NV knockout infectious hematopoietic necrosis virus expressing foreign genes, J. Virol. 74 (2000) 11247–11253.
[12] S. Biacchesi, The reverse genetics applied to fish RNA viruses, Vet. Res. 42 (2011) 12–20.
[13] P.J. Walker, R.G. Dietzgen, D.A. Joubert, K.R. Blasdell, Rhabdovirus accessory Genes 162 (2011) 110–125.
[14] Y.P. Chen, M.T. Guo, Y.X. Wang, X.J. Hua, S. Gao, Y.T. Wang, D.C. Li, et al., Immunity induced by recombinant attenuated IHNV (infectious hematopoietic necrosis virus)-G^{N438A} expresses *VP2* gene encoded IPNV (infectious pancreatic necrosis virus) against both pathogens in rainbow trout, J. Fish Dis. 42 (2019) 631–642.
[15] B. Dancho, M.O. Mckenzie, J.H. Connor, D.S. Lyles, Vesicular stomatitis virus matrix protein mutations that affect association with host membranes and viral nucleocapsids, J. Biol. Chem. 284 (2009) 4500–4509.
[16] C.S. Robison, M.A. Whitt, The membrane-proximal stem region of vesicular stomatitis virus G protein confers efficient virus assembly, J. Virol. 74 (2000) 2239–2246.
[17] M. Lorizate, H.G. Krausslich, Role of lipids in virus replication, Cold Spring Harb Perspect Biol 3 (2011) a004820.
[18] J. Votteler, W.I. Sundquist, Virus budding and the ESCRT pathway, Cell Host Microbe 14 (2013) 232–241.
[19] H.G. Gottlinger, T. Dorfman, J.G. Sodroski, W.A. Haseltine, Effect of mutations affecting the p6 gag protein on human immunodeficiency virus particle release, Proc. Natl. Acad. Sci. Unit. States Am. 88 (1991) 3195–3199.
[20] I.L. Blanc, M.C. Prévost, M.C. Dokhélar, A.R. Rosenberg, The PPPY motif of human T-cell leukemia virus type 1 Gag protein is required early in the budding process, J. Virol. 76 (2002) 10024–10029.
[21] B.A. Puffer, L.J. Parent, J.W. Wills JW, R.C. Montelaro, Equine infectious anemia virus utilizes a YXXL motif within the late assembly domain of the Gag p9 protein, J. Virol. 71 (1997) 6541–6546.
[22] H. Wang, K.M. Norris, L.M. Mansky, Analysis of bovine leukemia virus gag membrane targeting and late domain function, J. Virol. 76 (2002) 8485–8493.
[23] J. Yasuda, E. Hunter, A proline-rich motif (PPPY) in the Gag polyprotein of Mason–Pfizer monkey virus plays a maturation-independent role in virion release, J. Virol. 72 (1998) 4095–4103.
[24] B. Yuan, X. Li, S.P. Goff, Mutations altering the moloney murine leukemia virus p12 Gag protein affect virion production and early events of the virus life cycle, EMBO J. 18 (1999) 4700–4710.
[25] R.C. Craven, R.N. Harty, J. Paragas, P. Palese, J.W. Wills, Late domain function identified in the vesicular stomatitis virus M protein by use of rhabdovirus-retrovirus chimeras, J. Virol. 73 (1999) 3359–3365.
[26] A. Calistri, C. Salata, C. Parolin, G. Pal, Role of multivesicular bodies and their components in the egress of enveloped RNA viruses, Rev. Med. Virol. 19 (2009) 31–45.
[27] E.O. Freed, Viral late domains, J. Virol. 76 (2002) 4679–4687.
[28] A. Pincetic, J. Leis, The mechanism of budding of retroviruses from cell membranes, Advances in Virology 2009 (2009) 1–9.
[29] S.J. Martin, C.D. Perez, P.D. Bieniasz, Context-dependent effects of l domains and ubiquitination on viral budding, J. Virol. 78 (2004) 5554–5563.
[30] W.M. Henne, N.J. Buchkovich, S.D. Emr, The ESCRT pathway, Dev. Cell 21 (2011) 77–91.
[31] J.H. Hurley, P.I. Hanson, Membrane budding and scission by the ESCRT machinery: it's all in the neck, Nat. Rev. Mol. Cell Biol. 11 (2010) 556–566.
[32] B. Strack, A. Calistri, M.A. Accola, G. Palu, H.G. Gottlinger, A role for ubiquitin ligase recruitment in retrovirus release, Proc. Natl. Acad. Sci. Unit, States Am. 97 (2000) 13063–13068.
[33] B. Strack, A. Calistri, H.G. Gottlinger, Late assembly domain function can exhibit context dependence and involves ubiquitin residues implicated in endocytosis, J. Virol. 76 (2002) 5472–5479.
[34] L.L. Zhao, M. Liu, J.W. Ge, X.Y. Qiao, Y.J. Li, D.Q. Liu, Expression of infectious pancreatic necrosis virus (IPNV) VP2–VP3 fusion protein in Lactobacillus casei and immunogenicity in rainbow trouts, Vaccine 30 (2012) 1823–1829.
[35] C. Wang, G.H. Lian, L.L. Zhao, Y. Wu, Y.J. Li, L.J. Tang, et al., Virulence and serological studies of recombinant infectious hematopoietic necrosis virus (IHNV) in rainbow trout, Virus Res. 220 (2016) 193–202.
[36] R.D. Fisher, H.Y. Chung, Q. Zhai, H. Robinson, W.I. Sundquist, C.P. Hill, Structural and biochemical studies of ALIX/AIP1 and its role in retrovirus budding, Cell 128 (2007) 841–852.
[37] Y. Wu, M.T. Guo, X.J. Hua, K.X. Duan, G.H. Lian, L. Sun, et al., The role of infectious hematopoietic necrosis virus (ihnv) proteins in the modulation of NF-kB pathway during ihnv infection, Fish Shellfish Immunol. 63 (2017) 500–506.
[38] M.T. Guo, W. Shi, Y.X. Wang, Y.T. Wang, Y.P. Chen, D.C. Li, et al., Recombinant infectious hematopoietic necrosis virus expressing infectious pancreatic necrosis virus VP2 protein induces immunity against both pathogens, Fish Shellfish Immunol. 78 (2018) 187–194.
[39] S. Mi, X.W. Qin, Y.F. Lin, J. He, N.N. Chen, C. Liu, et al., Budding of tiger frog virus (an iridovirus) from HepG2 cells via three ways recruits the ESCRT pathway, Sci. Rep. 6 (2016) 26581.
[40] D.G. Demirov, E.O. Freed, Retrovirus budding, Virus Res. 106 (2004) 87–102.
[41] M.J. Landsberg, P.R. Vajjhala, R. Rothnagel, A.L. Munn, B. Hankamer, Three-dimensional structure of AAA ATPase vps4: advancing structural insights into the mechanisms of endosomal sorting and enveloped virus budding, Structure 17 (2009) 427–437.
[42] G.M. Taylor, P.I. Hanson, M. Kielian, Ubiquitin depletion and dominant negative VPS4 inhibit rhabdovirus budding without affecting alphavirus budding, J. Virol. 81 (2007) 13631–13639.
[43] A. Okumura, R.N. Harty, Rabies virus assembly and budding, Adv. Virus Res. 79 (2011) 23–32.
[44] B.J. Chen, R.A. Lamb, Mechanisms for enveloped virus budding: can some viruses do without an ESCRT? Virology 372 (2008) 221–232.
[45] L. VerPlank, F. Bouamr, T.J. LaGrassa, Tsg101, a homologue of ubiquitin-conjugating (E2) enzymes, binds the L domain in HIV type 1 Pr55Gag, Proc. Natl. Acad. Sci. U.S.A. 98 (2001) 7724–7729.
[46] A. Mamińska, A. Bartosik, M. Banach-Orłowska, I. Pilecka, K. Jastrzębsk, D. Zdżalik-Bielecka, et al., ESCRT proteins restrict constitutive NF-κB signaling by trafficking cytokine receptors, Sci. Signal. 9 (2016) ra8.
[47] J. Timmins, G. Schoehn, S. Ricard-Blum, S. Scianimanico, T. Vernet, R.W.H. Ruigrok, et al., Ebola virus matrix protein vp40 interaction with human cellular factors tsg101 and nedd4, J. Mol. Biol. 326 (2003) 493–502.
[48] T. Pawliczek, C.M. Crump, Herpes simplex virus type 1 production requires a functional escrt-iii complex but is independent of tsg101 and alix expression, J. Virol. 83 (2009) 11254–11264.
[49] B.G. Luttge, M. Shehu-Xhilaga, D.G. Demirov, C.S. Adamson, F. Soheilian, K. Nagashima, Molecular characterization of feline immunodeficiency virus budding, J. Virol. 82 (2008) 2106–2119.